Technical Notes

TECHNICAL NOTES are short manuscripts describing new developments or important results of a preliminary nature. These Notes cannot exceed 6 manuscript pages and 3 figures; a page of text may be substituted for a figure and vice versa. After informal review by the editors, they may be published within a few months of the date of receipt. Style requirements are the same as for regular contributions (see inside back cover).

Skin Friction Measurements Following Manipulation of a Turbulent Boundary Layer

V. D. Nguyen*
Laval University, Quebec, Canada
A. M. Savill†
University of Cambridge, England
and
R. V. Westphal‡
NASA Ames Research Center
Moffett Field, California

Nomenclature

C = logarithmic law intercept constant
C_f = skin friction coefficient, $C_f = \tau_w/(\frac{1}{2}\rho U_e^2)$
h = height of manipulator plate from wall
l,t = chord and thickness of flat-plate manipulator
Re_θ = Reynolds number based on momentum thickness, $Re_\theta = U_e\theta/\nu$
s = spacing between tandem mainpulators (measured between each leading edge)
U_τ = friction velocity, $U_\tau = \sqrt{\tau_w/\rho}$
U = mean velocity component in X direction
X,Y = right-hand Cartesian streamwise and vertical coordinate directions
δ = boundary-layer thickness
κ = von Kármán constant, $\kappa = 0.41$
ν,ρ = air kinematic viscosity and density
θ = boundary layer momentum thickness, $\theta = \int_0^\delta U/U_e(1-U/U_e)$
τ_w = skin friction
ξ = normalized streamwise coordinate, $\xi = (X-X_i)/\delta_i$
$(\ )_e$ = local freestream conditions
$(\ )_i$ = value at manipulator leading edge position
$(\ )_0$ = natural boundary layer (no manipulators)

Introduction to the Experiments

THE potential of flat-plate turbulence manipulators for reducing the overall viscous drag due to turbulent boundary layers on aerodynamic surfaces is presently being assessed. It is well known that some reduction in skin friction occurs locally downstream of such devices,[1,2] and estimates of the drag penalty incurred by the device can be made.[3] The latter may be viewed as the *cost* and the former as the *benefit* in defining a relevant figure of merit for such devices. Until recently, no *direct* measurements of *local* skin friction were available to aid in the accurate assessment of the benefit achieved from flat-plate manipulation of turbulent boundary layers. The purpose of the current Note is to present the results of three very recent experiments in which direct, local measurements of the skin friction reduction were obtained. The cost of obtaining these reductions in local skin friction (i.e., the device drag penalty) is not addressed here.

The three experiments to be discussed are summarized in Table 1. All have been carried out in relatively small wind tunnels at low subsonic freestream speeds and with nominally two-dimensional turbulent boundary layers approaching the manipulators. Static pressure was constant to within 0.5% of the freestream total pressure for experiments 2 and 3; a slight favorable pressure gradient (U_e increased by 7% over the test section) existed for experiment 1. For each experiment, the manipulator devices were thin, flat plates with $l \sim \delta_i$, held in tension parallel to the surface across the span of the tunnel. Based on the findings of previous experiments,[2,4] cases with a single plate and with tandem plates have been selected from the three experiments to match closely optimal values for plate geometry and placement.

Measurements of skin friction were obtained by direct, local methods in each case. The uncertainty for these measurements is estimated at 2–5% of the absolute C_f value, and is not dependent on boundary layer turbulence structure or two-dimensionality. For experiment 1, a small dual floating element of the nulling type was used.[1,4] The diameter of the floating element was 28.6 mm—about equal δ_i—and the instrument was mounted in a moveable plug and calibrated directly using small suspended weights. Measurements of mean velocity within the boundary layer were made using a pitot probe.

For experiment 2, a larger floating element (150 mm diam) was mounted at a fixed position in the wind tunnel.[2,5] This device was also of the null return type, employed a somewhat larger element (diameter $3\text{–}5\delta_i$), and was calibrated using small weights. Since the floating element was located at a fixed streamwise position, a varying manipulator position (changing X_i and h) was required to maintain h/δ_i approximately constant. A total head tube and crossed hot-wires were used to measure the mean velocity and Reynolds stresses.[5]

The laser oil film interferometer was used to obtain the skin friction measurements for experiment 3, and a total pressure probe and crossed hot-wires were used to measure the mean velocity and Reynolds stresses.[6] Since these experiments were performed at higher velocity, the use of supporting pins were required to prevent flutter of the plates.

Results and Discussion

Values of $C_{f,0}$ measured for experiments 1 and 3 (without manipulators) are shown for reference in Fig. 1. Values inferred by using the Preston tube or law-of-the-wall methods agreed with the direct measurements to well within 5%, which verified the uncertainty estimates made for the direct measurements. For experiment 2, $C_{f,0} = 0.00354$ was measured at the (fixed) balance position.

Received Dec. 13, 1985; revsion received June 30, 1986.

*Professor, Mechanical Engineering Department.
†Rolls-Royce Research Fellow, Cavendish Laboratory.
‡Aerospace Engineer. Member AIAA.

Table 1 Parameters for the three experiments

No.	Wind tunnel	U_e, m/s	Trip	X_i, mm	δ_i, mm	$Re_{\theta i}$	t, mm	l, mm	h/δ_i	l/δ_i	s/δ_i
1	61×46×480-cm inflow	16.0	None	71–88	20	2100	0.4	19.0	0.75	0.95	2.9–7.7
2	47×45×200-cm blower	11.2	4-mm-sq. bar, $X=0$	55–193	26–41	1900–3100	1.2	51–63.5	0.75–0.82	1.3–2.4	5.3–7.9
3	80×20×300-cm blower	27.5	0.4-mm wire, $X=20$ cm	112	17	3700	0.25	22.9	0.75	1.3	7.1

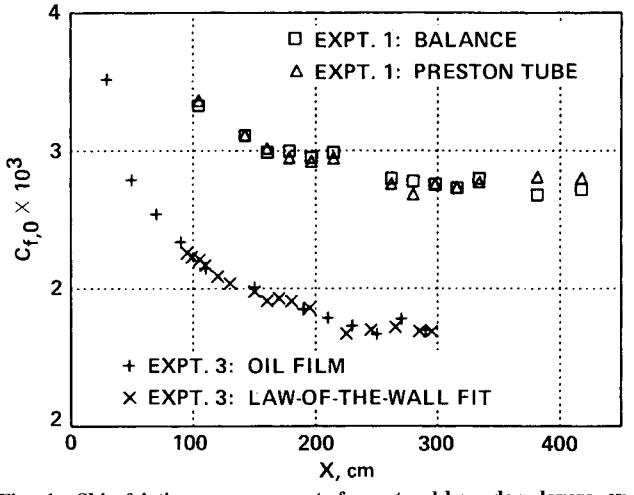

Fig. 1 Skin friction measurements for natural boundary layers, experiments 1 and 3. (Note shifted ordinate scale.)

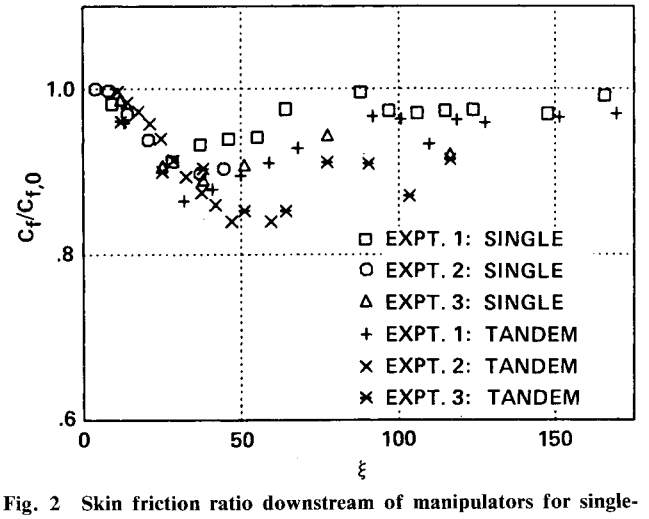

Fig. 2 Skin friction ratio downstream of manipulators for single- and tandem-plate devices.

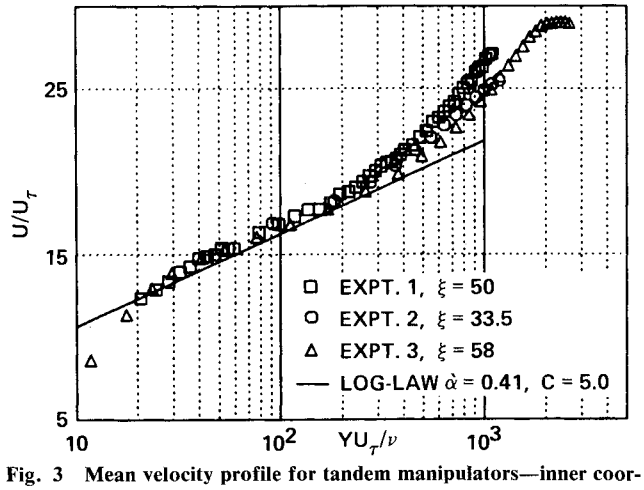

Fig. 3 Mean velocity profile for tandem manipulators—inner coordinates, U_τ from direct measurement.

Skin-friction data are presented in Fig. 2 for the cases of single- and tandem-plate manipulators. To accentuate the effect of the manipulators, the measured values for the manipulated cases have been divided by the value of $C_{f,0}$ at the same location and freestream conditions. Remarkably, the measurements agree reasonably well on all aspects of the downstream skin friction distribution, despite differences in the characteristics of the approach boundary layers and other experimental details. Initially, the skin friction drops downstream of both the single and tandem manipulators. The maximum measured reduction of skin friction was about 10% for each of the three experiments with single-plate devices, occurring at $\xi = 25$–50. Peak skin friction reductions of about 15% were achieved for the tandem devices at $\xi = 40$–60. Recovery is slow and there is as yet little data for $\xi > 100$, but it appears that the recovery process is essentially complete by about $\xi = 120$–150. No "overshoot" of the recovering skin friction above flat-plate values was observed in any of the experiments. The average reduction of surface skin friction over the surface extending to $\xi = 150$ was about 3–4% for single-plate manipulators, and about twice as much for the tandem configuration.

Mean velocity and skin friction measurements were used to examine the validity of the logarithmic law-of-the-wall for the maipulated boundary layers. Using the values of U_τ from direct measurement for the tandem-plate manipulators, Fig. 3 shows typical results from each experiment. The manipulated boundary layer displayed an accentuated wake, and a logarithmic region with nearly the same slope κ and slightly increased value of C compared to typical values for natural boundary layers. However, the magnitude of the upward shift is equivalent to less than 3% change in U_τ, or about 5–10% increase in C, and thus is probably not significant. Very near ($\xi < 10$) the manipulators, definite differences in profile similarity behavior were evident.[4,6]

Overall, the results suggest that, at best, only very small net drag reduction will be possible with optimized thin flat plates at moderate Re_θ because the maximum skin friction reduction is not large and is not sustained. Also, the profile similarity behavior was not significantly altered except very near the devices, further indicating that no overwhelming changes in turbulence transport properties have occurred due to manipulation. During revision of the present paper, the first direct measurements of the total drag of manipulators and the boundary layer compared with the boundary layer alone have been reported.[7] These results also indicated very little possibility for net drag reduction.

Acknowledgments

V. D. Nguyen would like to acknowledge the contributions of Messrs. J. Lemay, D. Provencal, R. Gourdeau, and Dr. J. Dickinson to the experiments carried out at Laval University. A. M. Savill is grateful for the assistance of Dr. J. C. Mumford in the work at Cambridge, which was supported by Rolls-Royce Ltd. under University Research Project 239.

References

[1]Nguyen, V. D., Dickinson, J., Jean, Y., Chalifour, Y., Anderson, J., Lemay, J., Haeberle, D., and Larose, G., "Some Experimental Observations of the Law of the Wall Behind Large-Eddy Breakup Devices Using Servo-Controlled Skin Friction Balances," AIAA Paper 84-0346, Jan. 1984.

[2]Mumford, J. C. and Savill, A. M., "Parametric Studies of Flat Plate, Turbulence Manipulators Including Direct Drag Results and

Laser Flow Visualization," *Proceedings of the New Orleans Conference on Laminar and Turbulent Boundary Layers*, ASME, New York, Feb. 1984, pp. 41-51.

[3]Govindaraju, S. P. and Chambers, F. W., "Direct Measurements of Drag of Ribbon Type Manipulators in a Turbulent Boundary Layer," AIAA Paper 86-0284, Jan. 1986.

[4]Lemay, J., Provencal, D., Gourdeau, R., Nguyen, V. D., and Dickinson, J., "More Detailed Measurements behind Turbulence Manipulators Including Tandem Devices Using Servo-Controlled Balances," AIAA Paper 85-0521, March 1985.

[5]Savill, A. M., "The Skin Friction Reduction Mechanisms of Flat Plate Turbulence Manipulators," *Proceedings of the EUROMECH 1984 Colloquium*, Saltsjobaden, Sweden, Aug. 1984.

[6]Westphal, R. V., "Skin Friction and Reynolds Stress Measurements for a Turbulent Boundary Layer Following Manipulation using Flat Plates," AIAA Paper 86-0283, Jan. 1986.

[7]Sahlin, A., Alfredsson, P. H., and Johansson, A. V., "Direct Drag Measurements for a Flat Plate with Passive Boundary Layer Manipulators," *Physics of Fluids*, Vol. 29, Feb. 1986, pp. 696-700.

Motion of Bubbles in a Varying Pressure Field

Michael Mond*
Ben-Gurion University of the Negev, Beer-Sheva, Israel

I. Introduction

RECENTLY, there has been a growing interest in the properties of bubbly liquids. This interest ranges from the propagation of sound waves in liquids to the properties of bubbly liquid metals for various technological applications.[1-3,8] The dynamics of compressible bubbles in a liquid exhibit variations on two distinct time scales under various conditions. This behavior is caused by the natural volume oscillations of the bubbles, which are much faster than the motion of the liquid. As a result, the time step used in numerical calculations of bubbly flows is limited by the low period of the fast oscillations. This limitation can be removed by separating the flow variables into slow and fast components. By analytically finding the fast behavior and integrating over it, the time step can be significantly increased and is limited only by the much slower motion.

The separation of the flow variables into fast and slow components is carried out by the multiple-scale analysis.[4] The slow variations in the oscillation period and amplitude of the bubbles are determined by the requirement that no secular terms exist in any order of the equations of motion.

In Sec. II the behavior of a single bubble in a slowly varying pressure field is investigated. In Sec. III the equations of motion of bubbly flow are separated into slow variables and fast oscillations. The resulting equations are averaged over the fast time scale.

II. Single-Bubble Dynamics

The equation describing the dynamics of a single bubble in an unbounded liquid is given by[5]

$$R\frac{d^2R}{dt^2}+\frac{3}{2}\left(\frac{dR}{dt}\right)^2=\frac{P_g-P_\infty}{\rho_1} \tag{1}$$

where R is the radius of the bubbles, P_g its internal pressure, ρ_1 is the density of the liquid, and P_∞ its pressure at infinity. It was assumed in Eq. (1) that the surface tension terms are small. Furthermore, in the case of a bubbly flow with a low gas content and small relative velocity between the bubbles and the liquid, Eq. (1) can still be used where P_∞ is replaced by the liquid's pressure next to the bubble P. Whereas Eq. (1) describes the fast oscillations of the bubbles that are on time scale t_b, the pressure P varies on a much slower time scale denoted by t_1. Thus Eq. (1) is given by

$$R\frac{d^2R}{dt^2}+\frac{3}{2}\left(\frac{dR}{dt}\right)^2=\frac{P_g-P(\tau)}{\rho_1} \tag{2}$$

where $\tau=\epsilon t$ and

$$\epsilon\approx t_b/t_1 \tag{3}$$

For a steady-state flow, ϵ can be estimated according to

$$\epsilon\approx\frac{u_b|\nabla P|}{P\omega_0} \tag{4}$$

where u_b and ω_0 are the velocity and natural frequency of the bubbles, respectively, and $P/|\nabla P|$ is an estimation of a characteristic length for a change in the liquid's pressure.

For the internal pressure P_g we use the equation of state of an ideal gas. Thus

$$P_g/\rho_1=a/R^3 \tag{5}$$

where a is a constant that depends on the temperature and the mass of the bubble. As was demonstrated by Plesset and Hsieh,[6] Eq. (5) holds for a wide range of frequencies.

Before turning to the multiple-scale analysis, we notice that since the bubble is expected to oscillate with a varying frequency, it is of benefit to define the following new variable:

$$\zeta=\int_0^t\omega_0(\epsilon\xi)d\xi=\frac{1}{\epsilon}\int_0^t\omega_0(\eta)d\eta \tag{6}$$

where the natural frequency is given by

$$\omega_0^2(\tau)=3a/R_0^3(\tau) \tag{7}$$

and $R_0(\tau)$ is obtained by setting the right-hand side of Eq. (2) to zero and using Eq. (5). The natural frequency at a constant pressure is obtained by linearizing Eq. (2) around a static state. After using the new independent variable defined by Eq. (6), Eq. (2) is transformed into the following equation:

$$R\frac{d^2R}{d\zeta^2}+\epsilon\frac{\omega_0'}{\omega_0^2}R\frac{dR}{d\zeta}+\frac{3}{2}\left(\frac{dR}{d\zeta}\right)^2=\frac{1}{\omega_0^2}\left(\frac{a}{R^3}-\frac{P}{\rho_1}\right) \tag{8}$$

where the prime denotes differentiation with respect to the argument.

We apply now the multiple-scale analysis. For this purpose we expand Eq. (8) in terms of the two time scales ζ and τ in the following way:

$$R(\zeta)=R_0(\tau)+\epsilon R_1(\zeta,\tau)+\epsilon^2R_2(\zeta,\tau)+\ldots \tag{9}$$

$$\frac{dR}{d\zeta}=\frac{\partial R}{\partial\zeta}+\frac{\epsilon}{\omega_0}\frac{\partial R}{\partial\tau} \tag{10}$$

$$\frac{d^2R}{d\zeta^2}=\frac{\partial^2R}{\partial\zeta^2}+2\frac{\epsilon}{\omega_0}\frac{\partial^2R}{\partial\zeta\partial\tau}+\frac{\epsilon^2}{\omega_0^2}\frac{\partial^2R}{\partial\tau^2} \tag{11}$$

Received June 8, 1986; revision received Oct. 1, 1986.

*Senior Lecturer, Pearlstone Center for Aeronautical Engineering Studies, Department of Mechanical Engineering.